

In Fig. 1.10.1 used is made as target of the single open shell spherical nucleus  $^{120}\text{Sn}$  lying along the stability valley, typical example of superfluid nuclei.

G - G

Capt. To Fig. 1.10.1

Version Feb. 26, 2016

88

## CHAPTER 1. INTRODUCTION

PP, I - IV  
handwritten

(2015) (see also Fig. 1.4.1).

In a very real sense this, namely the results collected in Fig. 1.10.1 is a nucleus. That is, the summed experimental and theoretical structural information accessed through (optical potential) asymptotic states, outcome of simultaneously probing the system with a complete array of experiments (elastic, anelastic and one- and two-nucleon transfer reactions), and of calculating the corresponding observables with an equally ample array of theoretical tools, as provided e.g. by NFT(s+r).

s+r

NFT (s+r)

## Appendix 1.A Confronting theory with experiment: absolute cross sections

In this appendix we provide a road map concerning the connection between theory and experiment<sup>76</sup> to be found in the present monograph, and in closely connected references.

### 1.A.1 One-particle transfer

#### Nuclei along the stability valley

Spectroscopic amplitudes and absolute cross sections,

- $^{120}\text{Sn}(p, d)^{119}\text{Sn}(7/2^+)$ : ~~Table 4.2.1~~, Fig. 4.2.1
- $^{120}\text{Sn}(d, p)^{121}\text{Sn}(j^\pi)(j^\pi = 11/2^-, 3/2^+, 1/2^+, 5/2^+, 7/2^+)$ : Table ~~4.2.1~~, Fig. 4.2.2
- $^{120}\text{Sn}(p, d)^{119}\text{Sn}((5/2^+); E_x)(E_x \leq 2 \text{ MeV})$ : ~~Table 4.2.2~~, Fig. 4.2.3

#### Optical potentials

Dickey, S. A. et al. (1982); Bechara, M. J. and Dietzsch (1975)<sup>77</sup>

#### Absolute differential cross sections: theory-experiment

~~Fig. 4.2.2 and 4.2.3.~~

#### Halo nuclei

- a)  $^9\text{Li}(d, p)^{10}\text{Li}(1/2^+)$
- b)  $^9\text{Li}(d, p)^{10}\text{Li}(1/2^-)$
- c)  $^{10}\text{Be}(d, p)^{11}\text{Be}$

<sup>76</sup>Physics is an experimental science: it is concerned only with those statements which in some sense can be verified by experiment (Schwinger (2001)).

<sup>77</sup>It is to be noted that, while no big differences are found, in all the transfer calculations involving medium heavy nuclei, the optical potentials collected in Table 6.2.2 were employed (Potel, G. et al. (2013)).

### Caption Fig 1.10.1

single-particle states and renormalizing the bare pairing interaction (I)

equations to propagate the variety of NFT processes dressing the  
the single open shell spherical nucleus

$^{120}\text{Sn}$  lying along the stability valley, provides  
 $^{50}$  an example of superfluid nuclei. This is

The reason why it has been studied extensively with a  
variety of <sup>this nucleus</sup> processes namely: elastic, anelastic (Coulomb excitation,  
and subsequent  $\gamma$ -decay, inelastic scattering), and  
one- and two-particle transfer reactions. The  
corresponding absolute differential cross sections and  
transition probabilities provide an essentially complete  
characterization of  $^{120}\text{Sn}$  involving as targets  
and residual systems the island of superfluid

nuclei  $^{118, 119, 120, 121, 122}\text{Sn}$  (see Idini et al (2015) <sup>PRC</sup>  
and refs. therein; see also Broglia et al (2016) <sup>Phys. Scr.</sup>  
(upper left), (color online) anelastic processes, Coulomb excitation,

and quadrupole  $\gamma$ -decay of  $^{119}\text{Sn}$  (middle left  
(a) experiment, (b) theory, (c) standard deviation  
between theory and experiment calculated as a  
function of the dynamical quadrupole deformation  
value  $\beta_2$  with respect to the experimental one ( $\beta_2$ )<sub>0</sub>;  
the corresponding values were used to draw the dashed  
orange curve of the center boxed landscape (i.e.  
Fig 1.4.1), see also Table 1.4.1);

**bold face**

(bottom left); Two-nucleon transfer processes  
(theoretical) (the absolute differential cross sections (continuous  
curves) associated with the reactions  $^{120}\text{Sn}(\text{pit})^{118}\text{Sn(g)}$   
and  $^{122}\text{Sn}(\text{pit})^{120}\text{Sn(g)}$ ) are displayed in (b)  
and (c); bottom middle, in comparison with the  
experimental data, while in connection with (d) these quantities  
were recalculated as a function of the coupling strength  
 $G$  with respect to the (equivalent) value  $G_0$  of  $\sqrt{\frac{1}{4}}$   
(Argonne  $^{150}$  bare NN-interaction and the corresponding  
standard deviation determined (only the values corresponding  
to  $^{120}\text{Sn}(\text{pit})^{118}\text{Sn(g)}$  are displayed)).

Caption Fig. (II)

It is of notice that the corresponding relative deviations  $\delta/L$ , where  $L = \exp. cross sections$  in this case (see Table 1.4.1) is  $70\mu b/2250\mu b \approx 0.03$  is quite small. This is in keeping with the fact that  $O \approx |\alpha_0|^2$ ,  $\alpha_0$  being the BCS order parameter (number of Cooper pairs participating in the condensate, <sup>which measure the</sup> deformation in gauge space). Because the state  $|BCS\rangle$  describing independent pair motion (Cooper pair condensate) is a coherent state displaying off-diagonal-long-range-order (ODLO), it is not surprising that  $|\alpha_0|^2 = \left| \sum_{V>0} U_V V_S \right|^2 = |\langle BCS | P^+ | BCS \rangle|^2 = |\langle BCS | P | BCS \rangle|^2$  plays the role of a physical, non-energy weighted sum rule <sup>\*)</sup> (~~Poté et al (2016)~~).

upper middle, (a) value of the <sup>state dependent</sup> pairing gap for the five valence orbitals of <sup>(blue line)</sup>  $^{120}\text{Sn}$  in comparison with the experimental findings ( $\Delta \approx 1.45 \text{ MeV}$ , arrow left). The gap associated with the lowest quasiparticle state  $n_{1/2}^{1/2}$  calculated as a function of  $m_K$  (different Skyrme interactions) as well as of  $G/G_0$  and  $\beta_2/\beta_2$ , have been calculated and the standard deviation with respect to the experimental findings reported (dotted blue curve, dashed brown curve, dashed green curve in the central figure);

\*) G. Poté et al (2017)

---

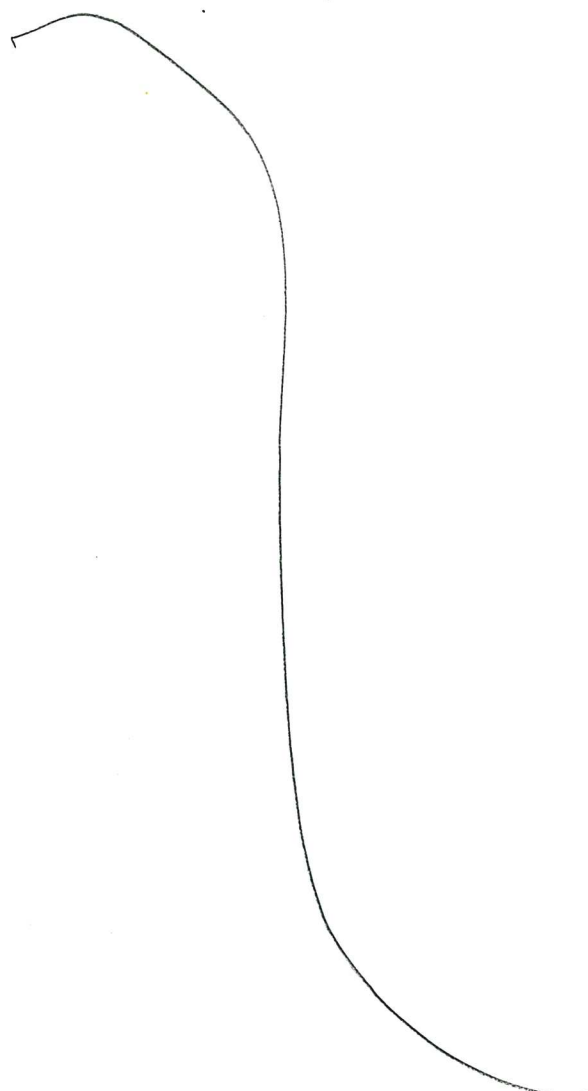
G. Poté, A. Idini, F. Barranco, E. Vigezzi and R.A. Broglia,  
From bare to renormalized order parameter in gauge space:  
structure and reactions

(right part): one-particle transfer processes processes  $^{120}\text{Sn}(\text{p},\text{d})^{119}\text{Sn}$  and  $^{120}\text{Sn}(\text{d},\text{p})^{121}\text{Sn}$ ;

Upper, (a) absolute differential cross sections associated with the low-lying states  $h^{11/2}$ ,  $d_{3/2}$ ,  $s_{1/2}$  and  $d_{5/2}$  populated in the reaction  $^{120}\text{Sn}(\text{d},\text{p})^{121}\text{Sn}$  (left) <sup>calculated</sup> (theory continuous curve, data solid dots); (b)  $^{120}\text{Sn}(\text{p},\text{d})^{119}\text{Sn}(5/2^+)$  absolute differential cross sections (continuous curves) in comparison with the experimental findings (<sup>right</sup> solid dots); also given are the DWBA fits used in the analysis of the experimental data; (c) comparison of the calculated strength function  $S_{5/2}$  ~~measured~~ with the data; (d) the difference between the centroid (width) of the experimental and calculated strength  $S_{05/2}$  is shown as a function of the ratio  $\beta_2/(\beta_2)_0$  in terms of the solid (dashed) curve; lower, the lowest quasiparticle quasiparticle energy values as a function of  $\beta_2/(\beta_2)_0$ ; (e) root mean-square deviation between the experimental and theoretical levels shown in (d) as a function of the ratio  $E/E_0$ . (f) The

IV

experimental energies of the members of the  $^{11/2}_\pi \otimes 2^+$  multiplet compared with the theoretical values, calculated as a function of the ratio  $\beta_2 / (\beta_2)_0$  (the root-mean-square deviation between the experimental and theoretical energies of the members of the  $^{11/2}_\pi \otimes 2^+$  multiplet shown in (g) as a function of ~~of~~  $\beta_2 / (\beta_2)_0$ )



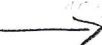
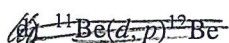
not yet written

- ${}^{10}\text{Be}(d,p){}^{11}\text{Be}$
- ${}^{11}\text{Be}(p,d){}^{10}\text{Be}$

90

Sect. 4.2.2 (corresponding  
Tables and Figs.)

Sect. 11



Optical potentials

Orrigo and Lenske

Y. Han, Y. Shi and Q. Shen, Phys. Rev. C 74 044615 (2006)

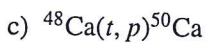
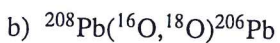
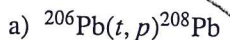
### 1.A.2 Two-particle transfer

J. Konings and J. P. Daloche,  
Nucl. Phys. A 713 (2003) 231

Nuclei along the stability valley

Closed shell nuclei

Spectroscopic amplitudes

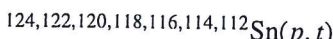


Optical potentials

Absolute differential cross sections: theory-experiment

Fig. 6.1.5

Open shell nuclei



Spectroscopic amplitudes

Table 6.2.1

~~Also the values associated with Sect. 6.2.3 [physical sum rule]~~

Optical potentials

Table 6.2.2

Absolute differential cross sections: theory-experiment

Fig. 6.2.1

**Nuclei around  $N = 6$  closed shell**

Spectroscopic amplitudes

- a)  ${}^1\text{H}({}^{11}\text{Li}, {}^9\text{Li}){}^3\text{H}$   
Eqs. (6.1.1)–(6.1.3)

- b)  ${}^7\text{Li}(t, p){}^9\text{Li}$

- c)  ${}^{10}\text{Be}(t, p){}^{12}\text{Be}$

**Optical potentials**

- a) Table 6.1.1

b) ref P. G. Young and R. H. Stokes, Phys. Rev. C4, 1597 (1971)

c) ref H. An and C. Cai, Phys. Rev. C73, 054605 (2006);  
H. T. Fortune, G. B. Liu and D. E. Alburger, Phys. Rev. C50, 1355 (1994),  
Absolute differential cross sections: theory-experiment

- a) Fig. 6.1.3

- b) Fig. 6.1.5

- c) Fig. 6.1.5



## Appendix 1.B Inelastic Scattering

In this Appendix we briefly discuss how to extract values of the effective deformation parameter  $\beta_L$  from inelastic scattering absolute differential cross sections in the most simple and straightforward way, ignoring all the complications associated with the spin carried by the particles, the spin-orbit dependence of the optical model potential, etc. The deformation parameter  $\beta_L$  enter e.g. the particle-vibration coupling Hamiltonian (Eqs. (1.3.8–1.3.13)).

### 1.B.1 $(\alpha, \alpha')$ -scattering

We start assuming that the interaction  $V'_\beta$  is equal to  $V'_\beta = V'_\beta(\xi_\beta, r_\beta)$ , which is usually called the stripping approximation. We can then write the differential cross section in the Distorted Wave Born Approximation (DWBA) as (see e.g. App 5.E) as,

$$\frac{d\sigma}{d\Omega} = \frac{k_\beta}{k_\alpha} \frac{\mu_\alpha \mu_\beta}{(2\pi\hbar^2)} |\langle \psi_\beta(\xi_\beta) \chi^{(-)}(k_\beta, \vec{r}_\beta), V'_\beta(\xi_\beta, r_\beta) \psi_\alpha(\xi_\alpha) \chi^{(+)}(k_\alpha, \vec{r}_\alpha) \rangle|^2. \quad (1.B.1)$$

For the case of inelastic scattering  $\xi_\alpha = \xi_\beta = \xi$ , thus

$$\psi_\beta(\xi_\beta) = \psi_{M_{l\beta}}^{I_\beta}(\xi) \quad (1.B.2a)$$

$$\psi_\alpha(\xi_\alpha) = \psi_{M_{l\alpha}}^{I_\alpha}(\xi) \quad (1.B.2b)$$

$$\vec{r}_\alpha = \vec{r}_\beta \quad \mu_\alpha = \mu_\beta, \quad (1.B.2c)$$

i.e we are always in the mass partition of the entrance channel.

Equation (1.B.1) can now be rewritten as

$$\frac{d\sigma}{d\Omega} = \frac{k_\beta}{k_\alpha} \frac{m_\alpha^2}{(2\pi\hbar^2)^2} \frac{1}{2I_\alpha + 1} \sum_{M_\alpha M_\beta} |\langle \chi^{(-)}(k_\beta, \vec{r}_\beta), V_{eff}(\vec{r}) \chi^{(+)}(k_\alpha, \vec{r}_\alpha) \rangle|^2, \quad (1.B.3)$$

where

$$\begin{aligned} V_{eff} &= \int d\xi \psi_{M_{l\beta}}^{I_\beta}(\xi) V'_\beta(\xi, \vec{r}) \psi_{M_{l\alpha}}^{I_\alpha}(\xi) \\ &= \int d\xi \psi_{M_{l\beta}}^{I_\beta}(\xi) V_\beta(\xi, \vec{r}) \psi_{M_{l\alpha}}^{I_\alpha}(\xi) \end{aligned} \quad (1.B.4)$$

as  $\psi^{I_\beta}$  and  $\psi^{I_\alpha}$  are orthogonal (remember  $V'_\beta = V_\beta - \bar{U}(r)$ ). We now expand the interaction in spherical harmonics, i.e.

$$\begin{aligned} V_\beta(\xi, \vec{r}) &= \sum_{LM} V_M^L(\xi, r) Y_M^L(\hat{r}) \\ &= \sum_{LM} V_M^L(\xi, \vec{r}). \end{aligned} \quad (1.B.5)$$

Defining

$$\int d\xi \psi_{M_{l\beta}}^{I_\beta}(\xi) [V_M^L(\xi, r) \psi^{I_\alpha}(\xi)]_{M_{l\beta}}^{I_\beta} = F_L(r), \quad (1.B.6)$$

we can write eq.(1.B.4) as

$$V_{eff}(\vec{r}) = \sum_{LM} (LMI_\alpha M_\alpha | I_\beta M_\beta) F_L(r) Y_M^L(\hat{r}). \quad (1.B.7)$$

Inserting (1.B.7) into (1.B.3) we obtain

$$\begin{aligned} \frac{d\sigma}{d\Omega} &= \frac{k_\beta}{k_\alpha} \frac{m_\alpha^2}{(2\pi\hbar^2)^2} \frac{1}{2I_\alpha + 1} \sum_{M_\alpha M_\beta} \left| \sum_{LM} (LMI_\alpha M_\alpha | I_\beta M_\beta) \right. \\ &\quad \times \left. \int d\vec{r} \chi^{(-)*}(k_\beta, \vec{r}_\beta) F_L(r) Y_M^L(\hat{r}) \chi^{(+)}(k_\beta, \vec{r}_\beta) \right|^2 \\ &= \frac{k_\beta}{k_\alpha} \frac{m_\alpha^2}{(2\pi\hbar^2)^2} \frac{2I_\beta + 1}{2I_\alpha + 1} \\ &\quad \times \sum_{LM} \frac{1}{2L + 1} \left| \int d\vec{r} \chi^{(-)*}(k_\beta, \vec{r}_\beta) F_L(r) Y_M^L(\hat{r}) \chi^{(+)}(k_\beta, \vec{r}_\beta) \right|^2, \end{aligned} \quad (1.B.8)$$

where we have used the orthogonality relation between Clebsch-Gordan coefficients

$$\begin{aligned} & \sum_{M_\alpha M_\beta} (LM I_\alpha M_\alpha | I_\beta M_\beta) (L' M I_\alpha M_\alpha | I_\beta M_\beta) \\ &= \sqrt{\frac{(2I_\beta + 1)^2}{(2L + 1)(2L' + 1)}} \sum_{M_\alpha M_\beta} (I_\beta - M_\beta I_\alpha M_\alpha | L - M) \\ & \quad \times (I_\beta - M_\beta I_\alpha M_\alpha | L' - M) = \frac{2I_\beta + 1}{2L + 1} \delta_{LL'} \end{aligned} \quad (1.B.9)$$

(fixed  $M$ )

Let us now discuss the case of inelastic scattering of even spherical nuclei.

The macroscopic Hamiltonian describing the dynamics of the multipole surface vibrations in such nuclei can be written, in the harmonic approximation as

$$H = \sum_{L,M} \left\{ \frac{B_L}{2} |\dot{\alpha}_M^L|^2 + \frac{C_L}{2} |\alpha_M^L|^2 \right\}, \quad (1.B.10)$$

where the collective coordinate  $\alpha_M^L$  is defined through the equation of the radius

$$R(\hat{r}) = R_0 \left[ 1 + \sum_{L,M} \alpha_M^L Y_M^{L*}(\hat{r}) \right], \quad (1.B.11)$$

and where  $R_0 = r_0 A^{1/3}$  fm.

The collective mode is generated from the interaction of the multipole field carried by each particle and the field of the rest of the particles. In turn this coupling modifies the single-particle motion. In particular the incoming projectile would feel this coupling. The potential  $V'_\beta$  is equal to

$$\begin{aligned} V'_\beta(\xi, \vec{r}) &= U(r - R(\hat{r})) \\ &= U(r - R_0 - R_0 \sum_{L,M} \alpha_M^L Y_M^{L*}(\hat{r})) \\ &= U(r - R_0) - R_0 \sum_{L,M} \alpha_M^L Y_M^{L*}(\hat{r}) \frac{dU(r - R_0)}{dr} \end{aligned} \quad (1.B.12)$$

$$= V_\beta(\xi, r) - \bar{U}_\beta(r)$$

$$\bar{U}_\beta(r) = -U(r - R_0)$$

$$V_\beta(\xi, \vec{r}) = R_0 \frac{d\bar{U}_\beta(r)}{dr} \sum_{L,M} \alpha_M^L Y_M^{L*}(\hat{r}) \quad \checkmark \quad (1.B.13)$$

Comparing with eq. (1.B.5) we obtain

$$V_M^L(\alpha, r) = R_0 \frac{d\bar{U}_\beta(r)}{dr} \alpha_{+M}^L \quad \checkmark \quad (1.B.14)$$

Note that  $H$  defined in Eq. (1.B.10) is the Hamiltonian of an  $L$ -dimensional harmonic oscillator, and that  $a_M^L$  is a classical variable. One can quantize this Hamiltonian in the standard way,

$$a_M^L = \sqrt{\frac{\hbar\omega_L}{2C_L}}(a_M^L - a_{-M}^{+L}), \quad (1.B.15)$$

where  $\hbar\omega_L$  is the energy of the vibration, and  $a_M^{+L}$  is the creation operator of a phonon. For an even nucleus

$$\begin{aligned} |\Psi_{M_\alpha}^{I_\alpha}\rangle &= |0\rangle \quad (I_\alpha = M_\alpha = 0), \\ |0\rangle &: \text{ ground (vacuum) state.} \end{aligned} \quad (1.B.16)$$

The one-phonon state can be written as,

$$\begin{aligned} |\Psi_{M_\alpha}^{I_\alpha}\rangle &= |I; LM\rangle = a_M^{+L}|0\rangle, \\ (I_\beta &= L; M_{I_\beta} = M). \end{aligned} \quad (1.B.17)$$

We can now calculate the matrix element of the operator (1.B.14), which connects states which differ in one phonon. Starting from the ground state we obtain

$$\begin{aligned} \langle I; LM | V_M^L(\alpha, r) | 0 \rangle &= (-1)^{L-M} R_0 \frac{d\bar{U}_\beta(r)}{dr} \sqrt{\frac{\hbar\omega_L}{2C_L}} \langle 0 | (a_M^L - a_{-M}^{+L}) | 0 \rangle \\ &= R_0 \frac{d\bar{U}_\beta(r)}{dr} \sqrt{\frac{\hbar\omega_L}{2C_L}} = -\frac{R_0}{\sqrt{2L+1}} \frac{d\bar{U}_\beta(r)}{dr} \beta_L \end{aligned} \quad (1.B.18)$$

where

$$\beta_L = \sqrt{\frac{(2L+1)\hbar\omega_L}{2C_L}}. \quad (1.B.19)$$

Substituting (1.B.18) into eq. (1.B.8) and making use of eqs. (1.B.16) and (1.B.17) we get

$$\begin{aligned} \frac{d\sigma}{d\Omega} &= \frac{k_\beta}{k_\alpha} \frac{\mu_\alpha^2}{(2\pi\hbar^2)^2} (\beta_L R_0)^2 \\ &\times \sum_M \frac{1}{2L+1} \left| \int d\vec{r} \chi^{(-)*}(k_\beta, \vec{r}) \frac{dU(r)}{dr} Y_M^{L*}(\hat{r}) \chi^{(+)}(k_\alpha, \vec{r}_\beta) \right|^2. \end{aligned} \quad (1.B.20)$$

Let us now assume that the nucleus has a permanent quadrupole ( $L = 2$ ) axially-symmetric deformation. For a  $K = 0$  band, the nuclear wave function has the form<sup>78</sup>

$$\Psi_{IMK=0} = \sqrt{\frac{2I+1}{8\pi^2}} \mathcal{D}_{M0}^I(\omega) \chi_{K=0} \quad (\text{intrinsic}), \quad (1.B.21)$$

<sup>78</sup> see e.g. Bohr, A. and Mottelson (1975) and refs. therein.

where we have used  $(\omega) = (\theta, \phi, \psi)$  to label the Eulerian angles which serve as orientation parameters.

In the intrinsic frame (which we take to coincide with the space-fixed axis when  $\theta = \phi = \psi = 0$ ) the nuclear surface has the shape

$$R(\hat{r}) = R_0 \left[ 1 + \sum_L b_L Y_0^L(\hat{r}) \right], \quad (1.B.22)$$

where the  $b_L$  introduced here is  $a_0^L$  in the intrinsic frame. When the nucleus has orientation  $\omega$ , this shape is rotated into

$$\hat{R}_\omega R(\hat{r}) = R_0 \left[ 1 + \sum_L b_L \mathcal{D}_{M0}^L(\omega) Y_0^L(\hat{r}) \right]. \quad (1.B.23)$$

One can then write,

$$W(r - R(\hat{r})) = W(r - R_0) - R_0 \frac{dW(r - R_0)}{dr} \sum_L b_L \mathcal{D}_{M0}^L(\omega) Y_0^L(\hat{r}), \quad (1.B.24)$$

which is the equivalent to Eq. (1.B.12) for the case of deformed nuclei. Then

$$V_M^L(b, r; \omega) = - \frac{d\bar{U}_\beta(r - R_0)}{dr} b_L \mathcal{D}_{M0}^L(\omega). \quad (1.B.25)$$

The effective interaction is now equal to

$$\begin{aligned} & \langle \Psi_{IMK=0}, V_M^L(b, r; \omega) \Psi_{000} \rangle = \\ & - R_0 \frac{d\bar{U}(r - R_0)}{dr} b_L \sqrt{\frac{(2L+1)^2}{8\pi^2}} \int d\omega \mathcal{D}_{M0}^{L*}(\omega) \mathcal{D}_{M0}^L(\omega) = \\ & - R_0 \frac{d\bar{U}(r - R_0)}{dr} b_L = - \frac{R_0}{\sqrt{(2L+1)}} \frac{d\bar{U}(r - R_0)}{dr} \beta_L = F_L(r) \end{aligned} \quad (1.B.26)$$

$(\beta_L = \sqrt{(2L+1)} b_L)$

in complete analogy to (1.B.18). Thus the same formfactor is used for both types of collective excitation. Within the above simple scheme of structure and reaction, the normalization factor  $(\beta_L R_0)^2$  is the only free parameter that can be obtained from the comparison of the experimental and theoretical (DWBA) differential cross section. The quantity  $\beta_L$  is known as the multipole deformation (dynamic or static) parameter, and gives a direct measure of the coupling of the projectile to the vibrational field. The value of  $\beta_L$  can also be obtained from the  $B(EL)$  reduced transition probability, in which case one has a measure of the electric moment, instead of the mass moment.

## Appendix 1.C Technical details NFT

In this Appendix we briefly discuss two technical aspects related to the overcompleteness of the basis used in NFT.

better scanning

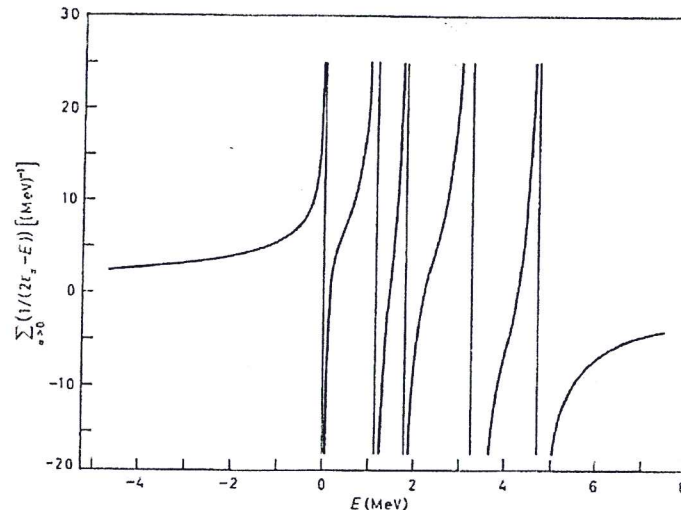


Figure 1.C.1: Dispersion relation for  $^{206}\text{Pb}$ . The single-hole states available to the two neutrons are  $p_{1/2}(0)$ ,  $f_{5/2}(0.57)$ ,  $p_{3/2}(0.89)$ ,  $i_{13/2}(1.63)$ ,  $f_{7/2}(2.34)$ . The label  $\alpha$  denotes the quantum numbers ( $j, m$ ).

### 1.C.2 Overlap

The states  $|\alpha\rangle$  and  $|\beta\rangle$  mix strongly through the couplings depicted by the graphs (a) and (b) of Fig. 1.7.10. Because of the energy dependence of the effective Hamiltonian (see (1.7.56), (1.7.57)) there is one matrix element for each state. The eigenvectors resulting from the diagonalization procedure were normalized according to (1.7.74). The corresponding amplitudes  $\xi_{iqm}$  (1.7.61) are displayed in Fig. 1.7.10 (e).

The normalization matrices  $\tilde{M}_{ii'}^{mm'}$  associated with the two  $3/2^+$  states discussed in Sect. 1.5 and 1.7, are given in Table 1.C.1. Details concerning the off-diagonal matrix elements are collected in Table 1.C.2.

It is of notice that in a conventional two-state model calculation implying a single matrix one would obtain

$$|I\rangle = A|\alpha\rangle + B|\beta\rangle$$

and

$$|II\rangle = -B|\alpha\rangle + A|\beta\rangle, \quad (1.C.6)$$

with  $A^2 + B^2 = 1$ . This model would predict the value  $R = (\alpha/\beta)^2$  for the  $(t, \alpha)$  ratio  $R(t, \alpha) = \sigma_I^{tr}/\sigma_{II}^{tr}$  and  $1/R$  for the  $(\alpha, \alpha')$  ratio  $R(\alpha, \alpha') = \sigma_I^{oct}/\sigma_{II}^{oct}$  (see Sect. 1.7.4). The ratio  $R_{th}(t, \alpha) = 1.83/2.25 = 0.81$  (against  $R_{exp}(t, \alpha) = 0.82$ ) and  $R_{th}(\alpha, \alpha') = 2.5$  (against  $R_{exp}(\alpha, \alpha') = 3.8$ ) is a direct consequence of the overcompleteness of the basis which is taken care of by the nuclear field theory. While this is a

$$\Rightarrow \left( \lim_{\omega_\alpha \rightarrow 0} \left( \frac{\hbar \omega_\alpha}{2 C_\alpha} \right)^{1/2} \right) = \lim_{\omega_\alpha \rightarrow 0} \left( \frac{\hbar^2}{2 D_\alpha \hbar \omega_\alpha} \right)^{1/2}$$

### 1.D. NFT AND REACTIONS

99

can be written as<sup>80</sup>,

$$H_{\text{coupl}} = \kappa \alpha F,$$

$H_c$

where

$$F = -\frac{1}{\kappa} \frac{\partial}{\partial x}, \quad (1.D.2)$$

and

$$\kappa = \int \frac{\partial}{\partial x} \frac{\partial \rho_0}{\partial x} d\tau = -A \left( \frac{\partial^2 U}{\partial x^2} \right), \quad (1.D.3)$$

corresponding to a normalization of  $\alpha$  such that  $\langle F \rangle = \alpha$ . It is of notice that both  $\kappa$  and  $A$  are negative for attractive fields (p. 356 of<sup>80</sup>)

The spectrum of normal modes generated by the field coupling (1.D.1), namely by a Galilean transformation of amplitude  $\alpha$ , contains an excitation mode with zero energy for which zero point fluctuations diverge in just the right way to restore translational invariance to leading order in  $\alpha$ . In fact, while the zero point fluctuations (ZPF)

$$\lim_{\omega_\alpha \rightarrow 0} \left( \frac{\hbar \omega_\alpha}{2 C_\alpha} \right)^{1/2} = \lim_{\omega_\alpha \rightarrow 0} \left( \frac{\hbar^2}{2 D_\alpha \hbar \omega_\alpha} \right)^{1/2} \quad (1.D.4)$$

diverges, the inertia remains finite and equal to  $D_\alpha = AM$ , as expected,  $C_\alpha$  being the restoring force constant

The additional dipole roots include, in particular, the isoscalar dipole modes associated with  $\hat{D} = \sum_{i=1}^A r_i^3 Y_{1\mu}(\hat{r}_i)$ , which can be viewed as a non-isotropic compression mode<sup>81</sup>.

Naturally, the operators leading to transformations associated with the change in the coordinates of relative motion (recoil effects) are Galilean operators ( $\sim \exp(k_{\alpha\beta} \cdot (r_\beta - r_\alpha))$ ). Their action (on e.g. the entrance channel), as that of (1.D.1) (on the shell model ground state), can be graphically represented in terms of NFT (or eventual extensions of them). In Figs 1.1.2 and 1.1.3 as well as 1.9.2–1.9.6 they are drawn in terms of jagged lines. How do we calculate such couplings? Let us elaborate on this point.

When one states that the small displacement  $\alpha$  of the nucleus leads to a coupling (1.D.1) one means a coupling between the single-particle and the collective displacement of the system as a whole. When one talks about the spectrum of normal modes associated with such a coupling, one refers to the harmonic approximation (RPA). Thus, to the solutions of the dispersion relation<sup>82</sup>,

$$-\frac{2\kappa}{\hbar} \sum_i \frac{|F|_i^2 \omega_i}{\omega_i^2 - \omega_a^2} = 1, \quad (1.D.5)$$

<sup>80</sup> See Bohr, A. and Mottelson (1975).

<sup>81</sup> See e.g. Colò et al. (2000).

<sup>82</sup> Bohr, A. and Mottelson (1975); Eq. (6-244), Brink D. and Braglia (2005), Sect. 8.3.1

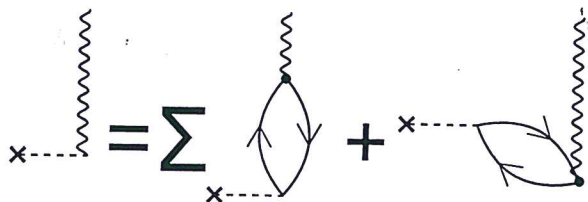


Figure 1.D.1: Self-consistent condition for normal modes

(dipole particle-hole excitations)

where the sum is over single-particle states. This dispersion relation can be represented graphically through the diagrams shown in Fig. 1.D.1. In particular,  $\alpha$  acting on the vacuum creates the collective mode. This can also be seen by expressing  $\alpha$  in second quantization, namely

$$\alpha = \sqrt{\frac{\hbar\omega_\alpha}{2C_\alpha}}(\Gamma_\alpha^\dagger + \Gamma_\alpha), \quad (1.D.6)$$

where  $\sqrt{\hbar\omega_\alpha/2C_\alpha} = \sqrt{\frac{\hbar^2}{2D_\alpha} \frac{1}{\hbar\omega_\alpha}}$  is the zero-point amplitude of the collective (displacement) mode. Now, none of the above arguments lose their meaning in the case in which there is a root with  $\omega_\alpha = 0$ , also in keeping with the fact the inertia remains finite. In Figs. 1.9.2–1.9.6 we do something similar to what is done in Fig. 1.D.1. The dot, which in this figure represents the particle-vibration coupling, is replaced by a small dashed open square, which we label “particle-recoil coupling vertex” (see labels Fig. 1.9.2). It constitutes a graphical mnemonic to count the degrees of freedom that are at play. In this case the coordinates of relative motion. Also the fact that in connection with the appearance of such vertices one has to calculate matrix elements of precise form factors which involve the recoil phases. As far as the actual calculation of a particle-mode vertex in which  $\omega_\alpha \rightarrow 0$ , an empirical way out is that of a coarse-grained-like symmetry restoration. In this case  $\kappa$  is adjusted in such a way, that the lowest solution of Eq. (1.D.5), although being smaller than the rest of them, remains finite.<sup>83</sup>

### 1.D.1 Potential scattering

The elastic differential cross section expressed in terms of partial waves is

$$\sigma(\theta) = |f(\theta)|^2 = \frac{1}{k^2} \left| \sum_{l=0}^{\infty} (2l+1) e^{i\delta_l} \sin \delta_l P_l(\cos \theta) \right|^2, \quad (1.D.7)$$

<sup>83</sup>Within this context we refer to Bohr, A. and Mottelson (1975), p. 446. With no coupling ZPF  $\alpha_0^{(0)}$  of the nuclear CM are small ( $\sim A^{-1/3}$ ). Thus, it is possible to tune  $\kappa$  so as to make the ZPF associated with the lowest root large as compared to  $\alpha_0^{(0)}$ , but still compatible with the ansatz at the basis of RPA (small amplitude harmonic vibrations).

Hc (Eq. (1.D.1)), the

where

$$f(\theta) = \frac{1}{2ik} \sum_{l=0}^{\infty} (2l+1) (e^{2i\delta_l} - 1) P_l(\cos \theta), \quad (1.D.8)$$

is the scattering amplitude. The total cross section

$$\sigma = 2\pi \int_0^\infty \sigma(\theta) \sin \theta d\theta = \frac{4\pi}{k^2} \sum_{l=0}^{\infty} (2l+1) \sin^2 \delta_l \quad (1.D.9)$$

expressed in term of  $f$ , namely,

$$\sigma = \frac{4\pi}{k} \Im f(0), \quad (1.D.10)$$

being a particular case of the optical theorem. The quantity  $\delta_l$  is known as the phase shift of the  $l$ th partial wave, namely the difference in phase between the asymptotic form of the actual radial wavefunction describing the scattering process and the radial wavefunction  $j_l(kr)$  in the absence of potential. The phase shifts which completely determine the scattering lead to a change in the scaling between incoming and outgoing waves which results, as expressed in (1.D.10), in the interference between them, so that particle intensity is smaller behind the scattering region ( $\theta \approx 0$ ) than in front of it. It is of notice that  $\delta_l$  cannot be measured directly. In fact, with the exception of the  $l = 0$  phase shift, obtained from low-energy scattering experiments, the values of  $\delta_l$  are inferred as empirical quantities from the parametrization of the potential. Even so, a degree of ambiguity concerning the uniqueness of the findings may remain.

*It is of notice that*

## 1.D.2 Transfer

We now consider a general reaction



in which the nucleus  $a$  impinges on the nucleus  $A$  in the entrance channel  $\alpha(a, A)$  and where the two nuclei in the exit channel  $\beta$ , namely  $b$  and  $B$  may differ from those in  $\alpha$ , by the transfer of one or more nucleons.

In the center-of-mass system, the total Hamiltonian may be written as

$$\begin{aligned} H &= T_{aA} + H_a + H_A + V_{aA}, \\ &= T_{bB} + H_b + H_B + V_{bB}, \end{aligned} \quad (1.D.12)$$

where  $T_{aA}$  is the kinetic energy of the relative motion in channel  $\alpha$

$$T_{aA} = -\frac{\hbar^2}{2m_{aA}} \nabla_{aA}^2, \quad (m_{aA} = \frac{m_a m_A}{m_a + m_A}), \quad (1.D.13)$$

in eq. (1.D.14) one obtains, assuming narrow wavepackets, product of an amplitude  $a_\beta(t)$  and a shape  $\chi_\beta(\mathbf{r} - \mathbf{R}_\beta(t), t)$ , ( $c_\beta = a_\beta \chi_\beta$ ),

$$\begin{aligned} & (\vec{\mathbf{r}}_\beta + \vec{\mathbf{r}}_\alpha)/2 \\ & i\hbar \sum_\beta \dot{a}_\beta(t) \langle \Psi_\xi | \Psi_\beta \rangle_{\mathbf{R}_\xi} e^{-iE_\beta t/\hbar} \\ & = \sum_\gamma \langle \Psi_\xi | V_\gamma - U_\gamma(r_\gamma) | \Psi_\gamma \rangle_{\mathbf{R}_\xi} a_\gamma(t) e^{-iE_\gamma t/\hbar}. \end{aligned} \quad (1.D.22)$$

where the sub-index on the matrix elements indicate that the integration over the degree of freedom of the two nuclei, the average center-of-mass coordinate  $\mathbf{r}_{\beta\gamma} = \frac{1}{2}(\mathbf{r}_\beta + \mathbf{r}_\gamma)$  should be identified with the average classical coordinate, i.e.

$$\mathbf{r}_{\beta\gamma} \rightarrow \mathbf{R}_{\beta\gamma} = \frac{1}{2}(\mathbf{R}_\beta + \mathbf{R}_\gamma). \quad (1.D.23)$$

The coupled equations (1.D.22) can be written in a more compact way by an orthogonalization procedure, which makes use of the adjoint channel wavefunctions

$$\omega_\xi = \sum_\gamma g_{\xi\gamma}^{-1} \Psi_\gamma, \quad (1.D.24)$$

where  $g^{-1}$  is the inverse of the overlap matrix

$$g_{\xi\gamma} = \langle \Psi_\xi | \Psi_\gamma \rangle, \quad (1.D.25)$$

that is

$$\sum_\xi g_{\gamma\xi} g_{\xi\beta}^{-1} = \sum_\xi g_{\gamma\xi}^{-1} g_{\xi\beta} = \delta(\gamma, \beta). \quad (1.D.26)$$

With this definition,

$$(\omega_\xi, \Psi_\beta) = \delta(\xi, \beta), \quad (1.D.27)$$

which takes care of non-orthogonality. Making use of the above relations one can rewrite (1.D.22) in the form

$$i\hbar \dot{a}_\beta(t) = \sum_\gamma \langle \omega_\beta | V_\gamma - U_\gamma | \Psi_\gamma \rangle_{\mathbf{R}_\beta} e^{i(E_\beta - E_\gamma)t/\hbar} a_\gamma(t) \quad (1.D.28)$$

By solving these coupled equations with the condition that at  $t = -\infty$  the system is in the ground state of  $a$  and  $A$  (entrance channel  $\alpha$ ), one can calculate the differential cross section

$$\frac{d\sigma_{\alpha \rightarrow \beta}}{d\Omega} = P_{\alpha \rightarrow \beta} \sqrt{\left( \frac{d\sigma_\alpha}{d\Omega} \right)_{el} \left( \frac{d\sigma_\beta}{d\Omega} \right)_{el}}, \quad (1.D.29)$$

(are involved in the determination of)

### 1.D. NFT AND REACTIONS

105

center-of-mass coordinate taking place when mass is transferred from one system to other. It gives rise to the recoil effect. Within the framework of DWBA it leads to a change of scaling of the DW (see also section elastic transfer). Summing up, the one-particle transfer amplitude reads

$$(a_\beta(t = +\infty))^{(1)} = \int_{-\infty}^{\infty} \langle \phi^{B(A)}(S^B(n), \mathbf{r}_{1A}), U_{1b}(r_{1b}) e^{\sigma_{\alpha\beta}} \phi^{a(b)}(S^a(n), \mathbf{r}_{1b}) \rangle_{R_{\alpha\beta}} \\ \times \exp \{i[(E_\beta - E_\alpha)t'/\hbar + \gamma_{\alpha\beta}]\} \quad (1.D.39)$$

While

In a similar way in which the phases  $\delta_l$  determine the elastic scattering cross section, in the present case it is the phase  $\delta_{\alpha\beta}$ . In fact,  $\delta_{\alpha\beta}$  determines the shift between incoming and outgoing waves and thus the interference process which is at the basis of the absolute value of the transfer differential cross section. In other words, the reaction part of the elastic and one-nucleon-transfer reaction cross section are embodied in  $\delta_l$  and  $\sigma_{\alpha\beta}$  respectively. The nucleon structure part is contained in the reduced mass  $\mu$  and potential  $U$  in the case of elastic scattering, and in the single-particle wavefunctions, potential  $U_{1b}$  and  $Q$ -value phase in the transfer case. Within the diagrammatic representation of particle-transfer reaction theory, the recoil phase is represented by a jagged line. Similar to  $\delta_l$ ,  $\sigma_{\alpha\beta}$  cannot be measured directly, but can in principle be inferred from the absolute cross section<sup>84</sup>.

nuclear

(differential)

the phases  $\delta_{\alpha\beta}$  play a similar role in the transfer process

<sup>84</sup>For more detail see Broglia and Winther (2004).

## BIBLIOGRAPHY

109

- ✓ R. A. Broglia. Microscopic structure of the intrinsic state of a deformed nucleus. Interacting Bose-Fermi systems in nuclei, page 95. Plenum Press, New York, 1981. Iachello, F., Ed.
- ✓ R. A. Broglia and A. Winther. *Heavy Ion Reactions*. Westview Press, Boulder, CO., 2004.
- ✓ R. A. Broglia, D. R. Bès, and B. S. Nilsson. Strength of the multipole pairing coupling constant. *Physics Letters B*, 50:213, 1974.
- ✓ R. A. Broglia, B. R. Mottelson, D. R. Bès, R. Liotta, and H. M. Sofía. Treatment of the spurious state in Nuclear Field Theory. *Physics Letters B*, 64:29, 1976.
- ✓ R. A. Broglia, P. F. Bortignon, F. Barranco, E. Vigezzi, A. Idini, and G. Potel. Unified description of structure and reactions: implementing the Nuclear Field Theory program. *Physica Scripta*, in press, 2016.
- ✓ Broglia, R. A. Heavy Ion Reactions. *Lecture notes, Brookhaven National Lab. (unpublished)*, 1979. *net adres*
- ✓ Broglia, R. A., J. S. Lilley, R. Perazzo, and W. R. Phillips. *Phys. Rev. C*, 1:1508, 1970.
- ✓ Broglia, R. A., V. Paar, and D. Bes. Diagrammatic perturbation treatment of the effective interaction between two-photon states in closed shell nuclei: The  $J^\pi = 0^+$  states in  $^{208}\text{Pb}$ . *Physics Letters B*, 37:159, 1971a.
- ✓ Broglia, R. A., V. Paar, and D. Bes. Effective interaction between  $J^\pi = 2^+$  two-phonon states in  $^{208}\text{Pb}$ . Evidence of the isovector quadrupole mode. *Physics Letters B*, 37:257, 1971b.
- ✓ Broglia, R. A., C. Riedel, and T. Udagawa. Sum rules and two-particle units in the analysis of two-neutron transfer reactions. *Nuclear Physics A*, 184:23, 1972.
- ✓ Broglia, R. A. and Zelevinsky, V. In R. A. Broglia and V. Zelevinsky, editors, *50 Years of Nuclear BCS*. World Scientific, Singapore, 2013.
- ✓ Broglia, R.A., O. Hansen, and C. Riedel. Two-neutron transfer reactions and the pairing model. *Advances in Nuclear Physics*, 6:287, 1973. URL [www.mi.infn.it/~vigezzi/BHR/BrogliaHansenRiedel.pdf](http://www.mi.infn.it/~vigezzi/BHR/BrogliaHansenRiedel.pdf).
- ✓ A. O. Caldeira and A. J. Leggett. Influence of dissipation on quantum tunneling in macroscopic systems. *Phys. Rev. Lett.*, 46:211, 1981.
- ✓ A. O. Caldeira and A. J. Leggett. Quantum tunneling in a dissipative system. *Ann. of Phys.*, 149:374, 1983.
- E. Chabanat, P. Bonche, P. Haensel, J. Meyer, and R. Schaeffer. A Skyrme parametrization from subnuclear to neutron star densities. *Nuclear Physics A*, 627:710, 1997.

write as  
ref. [196]  
*Phys. Scr.*  
(2016)

- ✓ G. Colò, N. V. Giai, P. F. Bortignon, and M. R. Quaglia. On dipole compression modes in nuclei. *Physics Letters B*, 485:362, 2000.
- ✓ Dickey, S. A., J. Kraushaar, R. Ristinen, and M. Rumore. The  $^{120}\text{Sn}(p, d)^{119}\text{Sn}$  reaction at 26.3 MeV. *Nuclear Physics A*, 377:137, 1982.
- ✓ H. Feshbach. Unified Theory of Nuclear Reactions. *Annals of Physics*, 5:357, 1958.
- ✓ R. Feynman. *Theory of fundamental processes*. Benjamin, Reading, Mass., 1975.
- ✓ Flynn, E. R., G. J. Igo, and R. A. Broglia. Three-phonon monopole and quadrupole pairing vibrational states in  $^{206}\text{Pb}$ . *Phys. Lett. B*, 41:397, 1972.
- ✓ Flynn, E.R. and Igo, G. and Barnes, P.D. and Kovar, D. and Bès, D. R. and Broglia, R.A. Effect of multipole pairing particle-hole fields in the particle-vibration coupling of  $^{208}\text{Pb}$  (II). The  $^{207}\text{Pb}(t, p)^{209}\text{Pb}$  reaction at 20 MeV. *Phys. Rev. C*, 3: 2371, 1971.
- ✓ Glendenning, N. K. *Direct nuclear reactions*. World Scientific, Singapore, 2004.
- ✓ W. Heisenberg. *The physical principles of quantum theory*. Dover, New York, 1949.
- ✓ A. Idini, G. Potel, F. Barranco, E. Vigezzi, and R. A. Broglia. Interweaving of elementary modes of excitation in superfluid nuclei through particle-vibration coupling: Quantitative account of the variety of nuclear structure observables. *Phys. Rev. C*, 92:031304, 2015.
- ✓ Idini, A., G. Potel, Barranco, E. Vigezzi, and R. A. Broglia. Dual origin of pairing in nuclei. *arXiv:1404.7365v1 [nucl-th]*, 2014.
- ✓ K. Kubo, R. Broglia, and T. Riedel, C. Udagawa. Determination of the  $Y_4$  deformation parameter from  $(p, t)$  reactions. *Phys. Lett. B*, 32:29, 1970.
- ✓ L. Landau. *Joun. Phys. USSR*, 5:71, 1941.
- ✓ W. A. Lanford. Systematics of two-neutron-transfer cross sections near closed shells: A sum-rule analysis of  $(p, t)$  strengths on the lead isotopes. *Phys. Rev. C*, 16:988, 1977.
- ✓ Mahaux, C., P. F. Bortignon, R. A. Broglia, and C. H. Dasso. Dynamics of the shell model. *Physics Reports*, 120:1–274, 1985.
- ✓ M. Mayer and J. Jensen. *Elementary Theory of Nuclear Structure*. Wiley, New York, NY, 1955.

title

p. 74